

Crystal structures and magnetic properties of 6H-perovskite-type oxides $\text{Ba}_3\text{M}\text{Ir}_2\text{O}_9$ ($M = \text{Mg}, \text{Ca}, \text{Sc}, \text{Ti}, \text{Zn}, \text{Sr}, \text{Zr}, \text{Cd}$ and In)

Takeshi Sakamoto, Yoshihiro Doi*, Yukio Hinatsu

Division of Chemistry, Graduate School of Science, Hokkaido University, Sapporo 060-0810, Japan

Received 17 November 2005; received in revised form 13 March 2006; accepted 8 April 2006

Available online 19 May 2006

Abstract

Crystal structures and magnetic properties of quaternary oxides $\text{Ba}_3\text{M}\text{Ir}_2\text{O}_9$ ($M = \text{Mg}, \text{Ca}, \text{Sc}, \text{Ti}, \text{Zn}, \text{Sr}, \text{Zr}, \text{Cd}$ and In) were investigated. Rietveld analyses of their X-ray diffraction data indicate that they adopt the 6H-perovskite-type structure with space group $P6_3/mmc$ or, in the case of $M = \text{Ca}, \text{Sr}$ and Cd , a monoclinically distorted structure with space group $C2/c$. The Ir valence configurations are $\text{Ba}_3\text{M}^{2+}\text{Ir}_2^{5+}\text{O}_9$ ($M = \text{Mg}, \text{Ca}, \text{Zn}, \text{Sr}$ and Cd), $\text{Ba}_3\text{M}^{3+}\text{Ir}_2^{4.5+}\text{O}_9$ ($M = \text{Sc}$ and In) and $\text{Ba}_3\text{M}^{4+}\text{Ir}_2^{4+}\text{O}_9$ ($M = \text{Ti}$ and Zr). Magnetic susceptibility and specific heat measurements were carried out. In the $\text{Ba}_3\text{M}^{2+}\text{Ir}_2^{5+}\text{O}_9$, the Ir^{5+} ions have a non-magnetic ground state and the magnetic behavior for these compounds is explained by the Kotani's theory. For $\text{Ba}_3\text{M}^{4+}\text{Ir}_2^{4+}\text{O}_9$, the effective magnetic moment of these compounds is significantly small, although the Ir^{4+} ions have magnetic moment, which indicates the existence of the strong antiferromagnetic interaction between Ir^{4+} ions in the $\text{Ir}_2^{4+}\text{O}_9$ face-shared bioctahedra. In the case of $\text{Ba}_3\text{M}^{3+}\text{Ir}_2^{4.5+}\text{O}_9$, a specific heat anomaly was found at about 10 K ($M = \text{Sc}$) and 1.6 K ($M = \text{In}$), which suggests the magnetic ordering of the magnetic moments of Ir^{4+} in the $(\text{Ir}^{4+}\text{Ir}^{5+})\text{O}_9$ bioctahedra.

© 2006 Elsevier Inc. All rights reserved.

Keywords: 6H-perovskite; Iridium; Rietveld analysis; Magnetic susceptibility; Specific heat

1. Introduction

The perovskite oxides ABO_3 form a wide family of compounds, reflecting the flexibility in the chemical composition and crystal structure. Generally, their structures can be regarded as the stacking of close-packed AO_3 layers and the filling of subsequent octahedral sites by B -site ions. The difference in the stacking sequence changes the way of linkage of BO_6 octahedra: the corner-sharing BO_6 in the ideal cubic perovskite (3C: three-layer and cubic) with $abc\dots$ sequence, the face-sharing BO_6 in 2H-perovskite (2H: two-layer and hexagonal) with $ab\dots$ sequence, and mixed linkages between the corner- and face-sharing in various intergrowth structures [1].

It is known that the B -site ions normally determine the physical properties of the perovskite oxides ABO_3 . Therefore, the perovskite-related oxides can show a variety of

physical properties reflecting the nature of the B -site cations and the linkage of BO_6 octahedra. The oxides containing platinum-group metals at the B -site often exhibit interesting magnetic and electronic properties. For example, Sr_2RuO_4 is a superconductor with $T_c \sim 1$ K [2], Sr_2IrO_4 shows weak ferromagnetic behavior below 250 K [3] and SrRuO_3 is a metallic ferromagnet below 160 K [4].

Recently, the 6H-perovskites containing platinum-group metals, $\text{Ba}_3\text{M}\text{M}'_2\text{O}_9$ ($M = \text{alkali metals, alkaline earth elements, } 3d \text{ transition metals, lanthanides; } M' = \text{Ru, Ir}$) [5–15] have been investigated. In those compounds, the stacking sequence of AO_3 layers is $ababc\dots$, and M and M' ions occupy the corner-sharing octahedral sites (MO_6) and the face-sharing octahedral ones ($\text{M}'_2\text{O}_9$ dimer), respectively. For many of these compounds, an antiferromagnetic spin-pairing occurs in the $\text{M}'_2\text{O}_9$ dimer even at room temperature. In the $\text{Ba}_3\text{NaRu}_2^{5.5+}\text{O}_9$ [10], the charge ordering between Ru^{5+} and Ru^{6+} ions (the formation of the $\text{Ru}_2^{5+}\text{O}_9$ and $\text{Ru}_2^{6+}\text{O}_9$ dimers) and the rapid decreasing of magnetic susceptibility were found below 210 K. In

*Corresponding author. Fax: +81 11 746 2557.

E-mail address: doi@sci.hokudai.ac.jp (Y. Doi).

addition, the $\text{Ba}_3MM'\text{Ir}_2\text{O}_9$ compounds show the magnetic transitions at low temperatures, which originate from the magnetic interaction between M and M' ions.

In this paper, we focused our attention on compounds $\text{Ba}_3M\text{Ir}_2\text{O}_9$ ($M = \text{Mg}, \text{Ca}, \text{Sc}, \text{Ti}, \text{Zn}, \text{Sr}, \text{Zr}, \text{Cd}$ and In). They are expected to adopt various charge configurations of $\text{Ba}_3M^{2+}\text{Ir}_2^{5+}\text{O}_9$ ($M = \text{Mg}, \text{Ca}, \text{Zn}, \text{Sr}$ and Cd), $\text{Ba}_3M^{3+}\text{Ir}_2^{4.5+}\text{O}_9$ ($M = \text{Sc}$ and In) and $\text{Ba}_3M^{4+}\text{Ir}_2^{4+}\text{O}_9$ ($M = \text{Ti}$ and Zr). All the M ions are non-magnetic in this case; thus, these compounds should show the characteristic magnetic behavior reflecting the different kinds of Ir_2O_9 dimers. We study systematically the crystallographic and magnetic properties of these compounds.

2. Experimental

2.1. Synthesis

Polycrystalline samples of compositions $\text{Ba}_3M\text{Ir}_2\text{O}_9$ ($M = \text{Mg}, \text{Ca}, \text{Sc}, \text{Ti}, \text{Zn}, \text{Sr}, \text{Zr}$ and In) were prepared by using standard solid-state techniques. As starting materials, BaCO_3 , MgO , CaCO_3 , Sc_2O_3 , TiO_2 , ZnO , SrCO_3 , ZrO_2 , In_2O_3 and Ir metal powders were used. They were weighed out in the appropriate metal ratios and well mixed in an agate mortar. The mixtures were pressed into pellets and then calcined at 900°C for 12 h. Subsequently, the products were annealed at 1000 – 1300°C for $12\text{ h} \times 5$ – 7 times with several interval regrindings and repelletings until a single $\text{Ba}_3M\text{Ir}_2\text{O}_9$ phase was obtained. Final heating temperatures were 1100°C ($M = \text{Ti}, \text{Zn}, \text{Sr}$), 1200°C ($\text{Mg}, \text{Ca}, \text{Zr}$), and 1300°C (Sc, In). For the preparation of $\text{Ba}_3\text{CdIr}_2\text{O}_9$, following starting materials were accurately weighed, i.e., $\text{BaO}_2\text{:CdO:IrO}_2\text{:Ir} = 3\text{:}1\text{:}1\text{:}1$, and were well mixed. The mixtures were ground and loaded in a platinum tube. The reaction was carried out in an evacuated quartz tube (to avoid the evaporation of CdO) at 1100°C for $12 \times 2\text{ h}$ with an interval grinding.

2.2. X-ray diffraction analysis

Powder X-ray diffraction patterns were collected with a Rigaku MultiFlex diffractometer using the monochromatic $\text{Cu-K}\alpha$ radiation in 2θ -steps of 0.02° and 7 s counting time in the range $10^\circ \leq 2\theta \leq 120^\circ$. The calculations were performed by the Rietveld method using the program RIETAN2000 [16]. The background and peak profiles were fitted by the Legendre polynomials and the split pseudo-Voigt function, respectively.

2.3. Magnetic susceptibility measurements

Magnetic susceptibility measurements were made in the temperature range of $1.8\text{ K} \leq T \leq 400\text{ K}$ using a SQUID magnetometer (Quantum Design, MPMS-5S). Data were collected under both zero-field-cooled (ZFC) and field-cooled (FC) conditions in an applied field of 0.5 T. For

$\text{Ba}_3\text{TiIr}_2\text{O}_9$, the field dependence of the magnetization was measured at 5 K in the $-5\text{ T} \leq H \leq 5\text{ T}$.

2.4. Specific heat measurements

Specific heat measurements were performed using a relaxation technique by a commercial heat capacity measuring system (Quantum Design, PPMS model) in the temperature range of 1.8–300 K. In the case of $\text{Ba}_3\text{InIr}_2\text{O}_9$, the specific heat was measured in the temperature range of 0.55–300 K. The sintered sample in the form of a pellet was mounted on a thin alumina plate with grease for better thermal contact.

3. Results and discussion

3.1. Crystal structures

The title compounds were prepared as a single phase except for $\text{Ba}_3\text{CdIr}_2\text{O}_9$, which contains a small amount ($\sim 1\%$) of unknown impurity. The X-ray diffraction profiles for $\text{Ba}_3\text{ZnIr}_2\text{O}_9$ and $\text{Ba}_3\text{SrIr}_2\text{O}_9$ are shown in Figs. 1 (a) and (b), respectively. The diffraction data for $M = \text{Mg}, \text{Sc}, \text{Ti}, \text{Zn}, \text{Zr}$ and In could be indexed with a hexagonal unit cell ($a_h \sim 5.8\text{ \AA}$, $c_h \sim 14\text{ \AA}$) and analyzed by the Rietveld method using a structural model for the 6H-perovskite $\text{Ba}_3\text{LnIr}_2\text{O}_9$ (space group $P6_3/mmc$) [17]. On the other hand, the data for $M = \text{Ca}, \text{Sr}$ and Cd show many diffraction peaks indexed with a larger orthohexagonal cell ($a \sim a_h$, $b \sim \sqrt{3}a_h$, $c \sim c_h$). Finally, all the diffraction peaks were explained by a monoclinic cell with space group $C2/c$, and successfully refined by using a structural

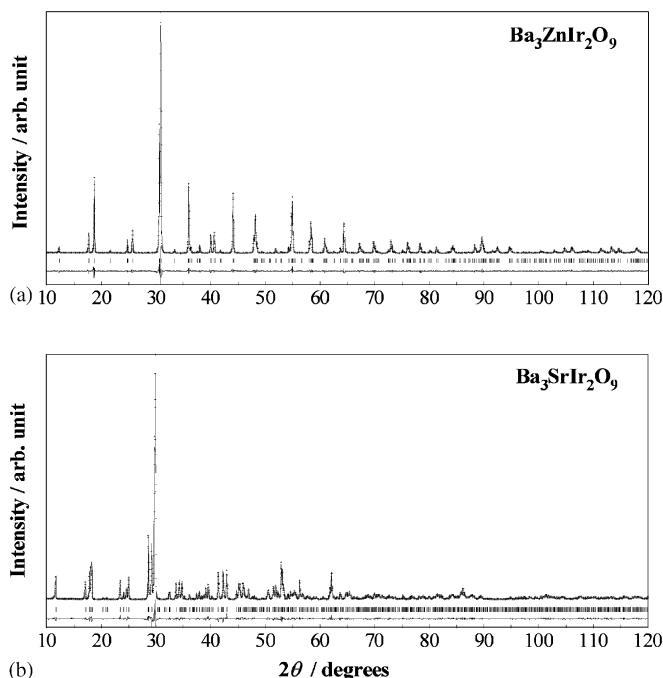


Fig. 1. X-ray diffraction profiles for (a) $\text{Ba}_3\text{ZnIr}_2\text{O}_9$ and (b) $\text{Ba}_3\text{SrIr}_2\text{O}_9$.

Download English Version:

<https://daneshyari.com/en/article/1333538>

Download Persian Version:

<https://daneshyari.com/article/1333538>

[Daneshyari.com](https://daneshyari.com)